




Photometric and Spectroscopic Analysis of LBV Candidate J004341.84+411112.0 in M31

A. Sarkisyan¹ , O. Sholukhova¹, S. Fabrika¹, A. Valeev^{1,2}, A. Valcheva³, P. Nedialkov³, and A. Tatarnikov⁴

¹ Special Astrophysical Observatory of Russian Academy of Sciences, Nizhny Arkhyz 369167, Karachai-Cherkessia, Russia; ars@sao.ru

² Crimean Astrophysical Observatory, Russian Academy of Sciences, Nauchnyi 298409, Russia

³ Department of Astronomy, Sofia University, 5 J. Bourchier Blvd, Sofia 1164, Bulgaria

⁴ Sternberg Astronomical Institute, Moscow M. V. Lomonosov State University, Universitetskiy Prospekt 13, Moscow 119234, Russia

Received 2021 August 26; revised 2021 October 28; accepted 2021 November 4; published 2022 January 21

Abstract

We study Luminous Blue Variable (LBV) candidate J004341.84+411112.0 in the Andromeda galaxy. We present optical spectra of the object obtained with the 6 m telescope of BTA SAO RAS. The candidate shows typical LBV features in its spectra: broad and strong hydrogen lines and the He I lines with P Cygni profiles. Its remarkable spectral resemblance to the well known LBV P Cygni suggests a common nature of the objects and supports LBV classification of J004341.84+411112.0. We estimate the temperature, reddening, radius and luminosity of the star using its spectral energy distribution. Obtained bolometric luminosity of the candidate ($M_{\text{bol}} = -10.41 \pm 0.12$ mag) is quite similar to those of known LBV stars in the Andromeda galaxy. We analyzed a ten year light curve of the object in *R* filter. The candidate demonstrates photometric variations of the order of 0.4 mag, with an overall brightness increasing trend $\Delta R > 0.1$ mag. Therewith, the corresponding color variations of the object are fully consistent with LBV behavior when a star become cooler and brighter in the optical spectral range with a nearly constant bolometric luminosity. LBV-type variability of the object, similarity of its spectrum and estimated luminosity to those of known LBVs allow us to classify J004341.84+411112.0 as an LBV.

Key words: stars: early-type – stars: massive – stars: variables: S Doradus – stars: Wolf Rayet – techniques: photometric – techniques: spectroscopic – galaxies: individual (KIC 8098300)

1. Introduction

In the present paper we report results of optical spectral and photometric monitoring of a Luminous Blue Variable (LBV) candidate in the Andromeda galaxy. We select object J004341.84+411112.0 from the list of LBV candidates by Massey et al. (2007, 2016a) for this study. The star was first discovered as an LBV candidate by Massey (2006) and was named by the author as a “P Cygni analog in M31” for its unique spectral similarity to one of the archetypes of LBVs, P Cygni. However, despite remarkable spectral resemblance to P Cygni, the author could not establish variability of the object and had to consider it as an LBV candidate. LBVs display various spectral features during the course of their life (Humphreys et al. 2014) and different types of brightness variation on different timescales (van Genderen 2001) which makes them difficult to classify. One of the main properties of an LBV is the presence of S Dor-type variability when a star becomes cooler and brighter in the optical spectral range with a nearly constant bolometric luminosity (Humphreys & Davidson 1994). Based on this, we try to demonstrate that the object J004341.84+411112.0 belongs to the class of LBV stars. Earlier we already studied J004341.84+411112.0 as a part of work on selected LBV candidates in

M31 (Sarkisyan et al. 2020). Here we continue and further our investigation with the help of extended long-term spectral and photometric observations. Below we analyze a ten year light curve of the object, describe its spectra, construct the spectral energy distribution (SED) and use it to determine the stellar parameters for the consequent classification. We will refer to the star by its first (R.A.) coordinate throughout the paper.

2. Observations

The optical spectra of J004341.84 were obtained with the SCORPIO spectrograph (Afasiev & Moiseev 2005) on the 6 m telescope BTA SAO RAS in October 2012, October 2019, September 2020 and October 2021. The observing log is displayed in Table 1. The spectra have been reduced using standard procedures for long-slit spectroscopy. They were bias and cosmic ray subtracted, co-added over multiple exposures, corrected for flat-field, and wavelength and flux calibrated. The spectral extraction was performed with the SPEXTRA code designed to work with stars in crowded fields (Sarkisyan et al. 2017).

Several photometric sets were also obtained with SCORPIO: in addition to the simultaneous spectral photometry, the object was also taken in January 2015 and September 2016.

Table 1
The Spectroscopic Observation Log

Date (DD.MM.YYYY)	Seeing (arcsec)	Exposition Time (s)	Grism	Spectral Range (Å)	Resolution (FWHM, Å)
15.10.2012	1.4	2 × 900	VPHG550G	3500–7200	11
16.10.2012	1.1	2 × 900	VPHG1200G	4000–5700	5.3
25.10.2019	1.5	2 × 1200	VPHG1200B	3600–5400	5.5
25.10.2019	1.5	2 × 600	VPHG1200R	5700–7500	5.3
28.09.2020	1.1	2 × 600	VPHG550G	3500–7200	11
28.09.2020	1.1	2 × 600	VPHG1200G	4000–5700	5.3
02.10.2021	2.2	4 × 900	VPHG1200B	3600–5400	5.5
02.10.2021	2.2	3 × 900	VPHG1200R	5700–7500	5.3

Note. The columns represent the date of the observations, average seeing, exposure time, grism used, spectral range and resolution in terms of full width at half maximum (FWHM).

Table 2
The Optical Photometry with SCORPIO and NIR Photometry with ASTRONIRCAM

Date	<i>U</i>	<i>B</i>	<i>V</i>	<i>R</i>	<i>I</i>
16.10.2012		18.10 ± 0.05	17.56 ± 0.05	17.17 ± 0.05	
17.01.2015		17.98 ± 0.08	17.48 ± 0.08	17.02 ± 0.05	16.81 ± 0.05
26.09.2016		17.80 ± 0.05	17.35 ± 0.05	16.88 ± 0.05	
25.10.2019		17.92 ± 0.05	17.40 ± 0.05	17.03 ± 0.04	
28.09.2020	17.45 ± 0.08	17.87 ± 0.09	17.44 ± 0.04	17.01 ± 0.04	16.79 ± 0.09
02.10.2021	17.44 ± 0.10	17.89 ± 0.06	17.34 ± 0.04	17.93 ± 0.03	16.62 ± 0.12
		<i>J</i> _{MKO}	<i>H</i> _{MKO}	<i>K</i> _{MKO}	
18.12.2018		16.32 ± 0.05	16.09 ± 0.05	15.80 ± 0.05	

Note. We show the date of the observations and estimated magnitudes with their uncertainties.

Magnitudes of the object were estimated by comparison with nearby stars in the field, with the help of the Local Group Galaxy Survey (LGGs, Massey et al. 2016b) calibration. Results of the optical photometry with SCORPIO are given in Table 2.

The additional optical photometric data of the object have been acquired with the 50/70 cm Schmidt telescope at NAO Rozen, Bulgaria which was equipped with an FLI 4096 × 4096 pix CCD camera with a scale of 1".07 pix⁻¹. The observations cover a period of 3 yr (2016 July 9–2019 July 8) and contain mainly *R* and *B* band images and only 7 epochs in *V* band. The seeing conditions were between 2" and 4" with a typical value of 2".5. The raw images were darkfield subtracted and flatfielded using standard IRAF (Tody 1986, 1993) routines. The images of a given night in each band were aligned and combined (usually 3 × 300 or 5 × 300 s) and an aperture photometry of the object of interest and the standard calibration stars was done by IRAF/DAOPHOT package (Stetson 1987; Stetson et al. 1990) with aperture radius around FWHM of the image. We relied on the LGGs catalog (Massey et al. 2016b) for standard calibration of our instrumental magnitudes.

Near-infrared (NIR) photometric observations of the object were carried out using the ASTRONIRCAM camera (Nadjip et al. 2017) attached to the 2.5 m telescope at the Caucasus Mountain Observatory of Sternberg Astronomical Institute (Shatsky et al. 2020). Observations were performed using the dithering method, with the telescope shifting between frames by 5". All frames were corrected for nonlinearity, dark current and flat field. For *JHK* photometry, we utilized summary images with effective exposures of 780, 840 and 930 s, respectively. The stars 2MASS J00433931+4111319 and J00433889+4111202 were used as comparison stars for calibration. Their brightnesses were taken from the 2MASS catalog (Cutri et al. 2012) and converted into the MKO photometric system (Simons & Tokunaga 2002; Tokunaga et al. 2002; Tokunaga & Vacca 2005) referencing the color equations from Leggett et al. (2006).

3. Spectra

Figure 1 depicts optical the spectra of our star. In addition to the spectrum of 2012 from Sarkisyan et al. (2020), here we present the spectra of 2019, 2020 and 2021.

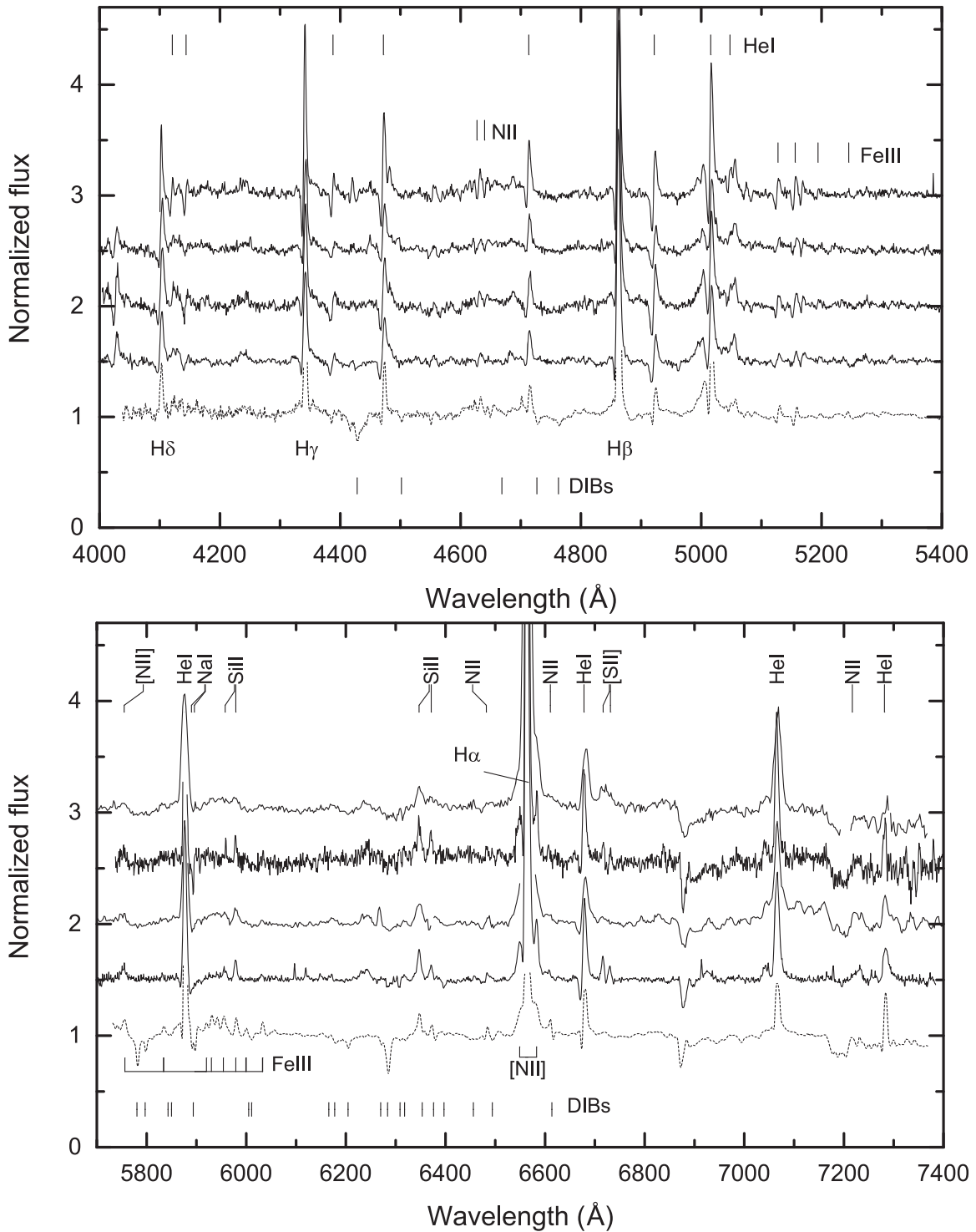


Figure 1. The optical spectra of J004341.84 and MN112. The solid lines represent spectra of J004341.84 from October 2012, October 2019, September 2020 and October 2021 epochs (from top to bottom respectively). The spectrum of the MN112 from Sarkisyan et al. (2020) is shown with a dotted line for comparison. The principal strong lines and diffuse interstellar bands (DIBs) are identified.

We also show the spectrum of the Galactic LBV candidate MN112 from Sarkisyan et al. (2020). We used the MN112 spectrum for comparison since it is almost identical to the spectrum of the well known LBV P Cygni (Gvaramadze et al. 2010; Kostenkov et al. 2020). Figure 1 clearly reveals that all the spectra of J004341.84 are extremely similar to the spectrum of MN112 and consequently, to that of P Cygni. One can directly compare our spectra with the spectrum of P Cygni from Stahl et al. (1993): the spectrum of J004341.84, like P Cygni, is dominated by strong emission lines of hydrogen and He I; the Balmer lines have wide wings and weak P Cygni absorption components, while the He I and Fe III lines show strong P Cygni profiles, and numerous emission lines of Fe III, Si II and N II are also present.

Both the stars J004341.84 and MN112 have P Cygni profiles in hydrogen, He I and Fe III lines, and their spectroscopic similarity with the bona fide LBV P Cygni is evident. This remarkable spectral resemblance of the star to P Cygni suggests a common nature of the objects, which is a decent argument in support of LBV classification of J004341.84.

Our spectra confirm previous classification of the object as an Of/late-WN star (Massey et al. 2007; Humphreys et al. 2014). However, we would like to draw attention to the following features of our spectra: P Cyg profiles of hydrogen lines, lack of N III 4634-40-42 lines, characteristics of a Of/late-WN star and quite weak He II 4686 line, one of the distinctive lines for Of/late-WN stars. Moreover, during our monitoring we noted variation of the He II 4686 line. Figure 2 demonstrates the significant weakening of the He II 4686 line from 2012 to 2019 and the reverse strengthening from 2019 to 2020 and 2021. Similar disappearing of the He II 4686 line was demonstrated by two Of/late-WN stars, R127 (Stahl et al. 1983) and HDE 269 582 (Stahl 1986), that subsequently have been classified as LBVs (Walborn et al. 2017). So, we tend to think that this behavior of the object points to its LBV instability.

4. Spectral Energy Distribution

For our LBV candidate J004341.84, we follow the method of determining the fundamental parameters of LBVs developed by us using an example of AE And and Var A-1 and new LBVs that we discovered (Sholukhova et al. 2015; Sarkisyan et al. 2020). The method is based on modeling LBV SEDs related to different states of a star, taking into account the intrinsic property of LBV stars—changing brightness in the optical spectral range with a nearly constant bolometric luminosity (Humphreys & Davidson 1994). The well known problem of A_V - T parameter degeneracy may therefore be solved, since the constant bolometric luminosity and interstellar extinction for different LBV states allow us to constrain model parameters (Sholukhova et al. 2011, 2015). As will be seen in Section 5,

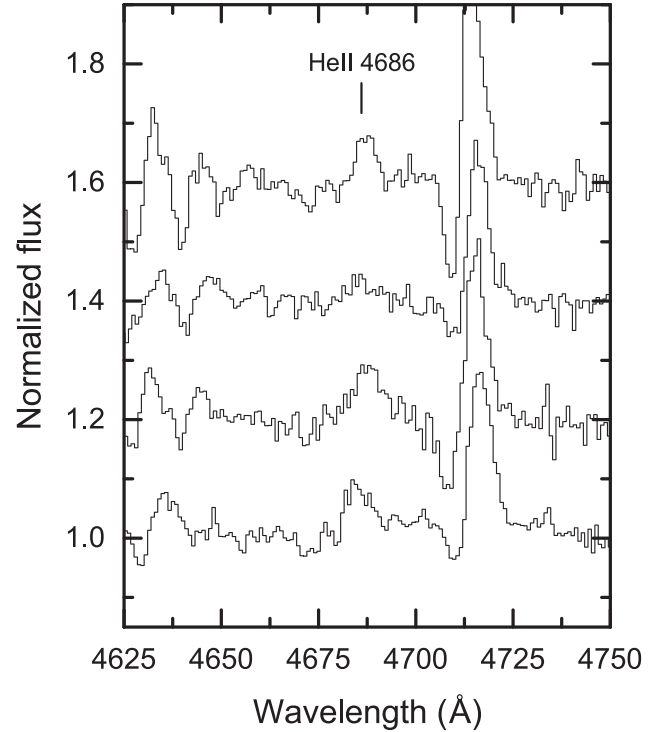


Figure 2. The optical spectra of the J004341.84 in the region of the He II 4686 line. The order of the spectra is the same as in Figure 1. The He II 4686 line significantly weakened from 2012 to 2019 and then strengthened again from 2019 to 2020 and 2021.

our object J004341.84 manifests LBV-type variability, which enables us to apply the method.

We start with preliminary estimates of stellar temperature (T_{sp} in Table 3) using the visibility of lines in the spectra. Since the spectra of the object do not show significant variations at SCORPIO resolution, we define the T_{sp} range as 18,000–22,000 K for all epochs. Next, we fit the photometric data points with a blackbody spectrum using the constrained temperature and taking into account the dust extinction (Fitzpatrick 1999) with $R_V = 3.1$. Following this way, we fit five different sets of photometric data obtained with SCORPIO (see Table 2), setting bolometric luminosity and extinction to be constant for all sets, and estimate stellar parameters in corresponding states.

Figure 3 depicts the SED and its modeling result for our star. We used the optical photometry with SCORPIO and NIR photometry with the ASTRONIRCAM (Table 2) for SED construction. To avoid cluttering the figure, only the data from the 2012, 2018, 2020 and 2021 epochs and spectrum from 2012 are displayed. We use the $UBVRI$ spectral range only for an approximation because the model does not take into account contribution from the bremsstrahlung radiation and dust emission. We subtract emission line contribution from the

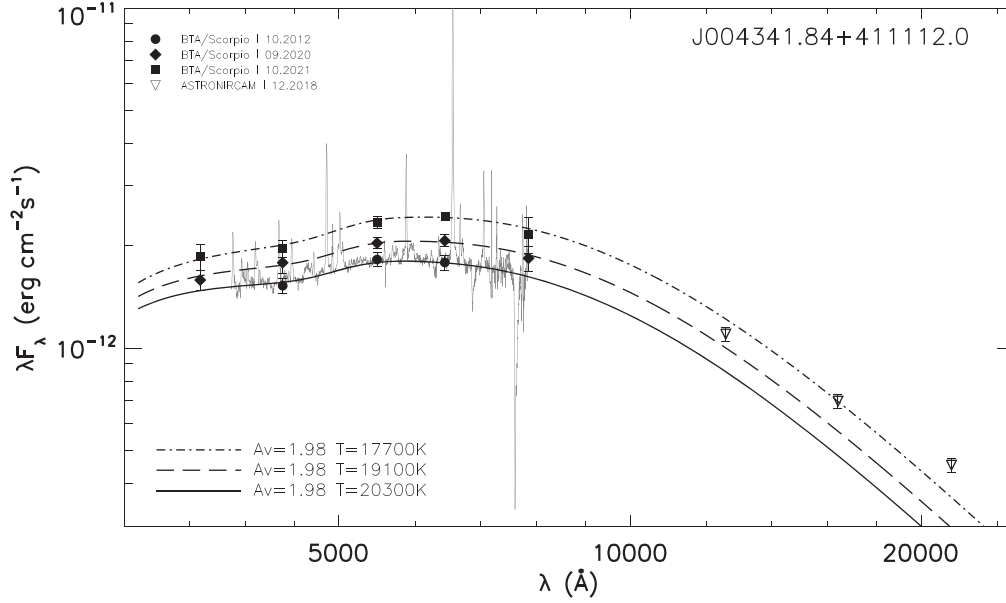


Figure 3. The SEDs of J004341.84 in the optical and NIR ranges. Only the photometric data for 2012, 2018, 2020 and 2021 epochs and spectrum from 2012 are shown to avoid cluttering the figure. The filled symbols designate the approximate data sets corrected for the emission lines and spectral slope. The model spectra are shown with solid (for the 16 October 2021 epoch), dashed (for the 28 September 2020 epoch) and dash–dotted (for the 2 October 2021 epoch) lines. The legends in the figure indicate object name, symbols, instruments and dates for the photometry and the best fitting parameters of temperature and reddening.

Table 3
SED Fitting and Estimated Parameters for J004341.84

Date	T_{sp} (K)	T_{SED} (K)	A_V (mag)	R (R_{\odot})	M_{bol} (mag)
16.10.2012		$20,300 \pm 370$		87 ± 5	
17.01.2015		$19,300 \pm 370$		96 ± 3	
26.09.2016	17,000–22,000	$18,000 \pm 400$	1.98 ± 0.06	110 ± 4	-10.41 ± 0.12
25.10.2019		$19,000 \pm 350$		99 ± 4	
28.09.2020		$19,100 \pm 330$		98 ± 4	
02.10.2021		$17,700 \pm 300$		114 ± 4	

Note. The columns show the date of photometric data used for SED fitting and indicating the state of the object, stellar photosphere temperature estimated from the spectrum, temperature and reddening A_V estimated from the SED fitting, stellar radius, M_V and M_{bol} . Values of the columns T_{sp} , A_V and M_{bol} are common for all epochs (see text of Section 4).

photometric points using our spectra and apply corrections to the effective band wavelengths for the spectral slope. Photometric points with those corrections are marked with the filled symbols in Figure 3. NIR photometric points were not used for fitting and are shown without any corrections by open symbols. The results of the SED approximation are signified with solid, dashed and dash–dotted lines for the 2012, 2020 and 2021 epochs, respectively. The SED fitting results for remaining epochs are presented in Table 3, which shows best-fitting parameters and based on them estimated parameters: A_V , temperature, radius and bolometric magnitude M_{bol} . We have to note that we accepted the distance to M31 of 752 ± 27 kpc (Riess et al. 2012) in our calculation.

The method allows us to estimate A_V with appropriate accuracy, and therefore to estimate the bolometric luminosity of the star. Obtained values of extinction and luminosity match the estimates of Massey (2006) well, and luminosity value corresponds to that of known LBVs in M31 (Humphreys et al. 2014). Position of J004341.84 on the Hertzsprung–Russell (HR) diagram is marked in Figure 4. The object lies in the immediate proximity of the S Dor instability strip (Wolf 1989) and is remarkably close to P Cyg and R127.

The *JHK* photometric points on the SED clearly show small NIR excess. However the shape of excess and its not particularly outstanding value in *K* filter indicate that it relies on contribution of free–free (f–f) but not warm dust emission.

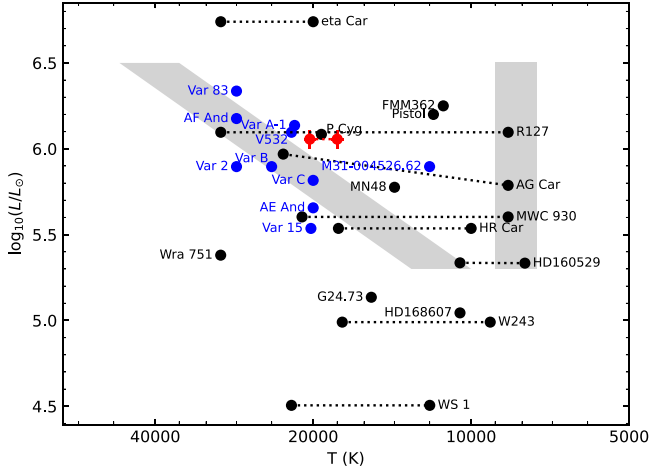


Figure 4. Position of J004341.84 on the HR diagram. LBVs in M31 and M33 are shown with blue points according to the data from the work of Humphreys et al. (2017a). Positions of the Galactic LBVs and R127 are taken from a similar figure in Smith et al. (2019) and marked in black. The position of J004341.84 based on its SED modeling in current work is shown in red. The gray boxes signify the locations of the S Dor instability strip (Wolf 1989) and the constant temperature strip of LBVs in outburst.

This excludes the possibility to classify the object as a B[e] supergiant (Humphreys et al. 2017b). Furthermore, according to Spitzer/IRAC photometry (Rafiei Ravandi et al. 2016) the object has color index $[3.6] - [4.5] = 0.212$ (based on isophotal magnitudes from the catalog), which corresponds to the LBV region on the diagram as suggested by Humphreys et al. (2017b, Figure 6(b)).

5. Photometry and Light Curve

In Figure 5 we present a compiled light curve of J004341.84 in R band constructed from our and archive data for the period from 2010 to 2021. In addition to our data we also use photometric data from Panoramic Survey Telescope and Rapid Response System (Pan-STARRS, Chambers et al. 2016) and data from the work of Martin & Humphreys (2017). To adopt data from the Pan-STARRS archive we utilize equations for photometric transformations between Pan-STARRS and other systems from the work of Tonry et al. (2012). The vertical lines indicate the dates that the spectra were obtained on the BTA telescope.

To confirm object variability we apply the median which is a robust statistic as the variability index (Enoch et al. 2003; Rose & Hintz 2007): $\bar{\eta} = \frac{1}{N-1} \sum_{i=1}^N \left| \frac{m_i - \bar{m}}{\sigma_i} \right|$. For a constant star, the value would be close to unity whereas stars with values above 1 are regarded as photometrically variable objects. The calculated value for our light curve is $\bar{\eta} = 3.59$. The object shows a variability range $\Delta R \approx 0.4$ mag. Despite the brightness variation not being outstanding, the light curve clearly features an increasing brightness trend over the last decade with

$\Delta R > 0.1$ mag and it is quite enough to classify the candidate as an LBV in quiescent phase (van Genderen 2001).

Moreover, the color variations of the object strongly support the LBV classification. As we see from Figure 5, the $(V - R)$ color becomes redder with time and, more importantly, a brightness increase, corresponding to an actual temperature decrease. This is fully consistent with LBV behavior when a brightness increase occurs as the temperature decreases due to radius inflation, while the object's bolometric luminosity stays roughly constant (Humphreys & Davidson 1994). Since this feature is distinctive to S Doradus variables (Lamers et al. 1998; van Genderen 2001), the light curve of J004341.84 and its color variations confirm the LBV classification of the object.

6. Conclusions

We study the LBV candidate J004341.84 using our spectra and photometry as well archival photometric data. In order to confirm the LBV status of the star we analyzed the light curve of this object in R filter and estimated the stellar parameters from the SED of the object.

Massey et al. (2007) and Humphreys et al. (2014) classify this LBV candidate as an Of/late-WN star. A connection between the Of/late-WN and LBV classes has been established by the transition of one of the prototypes of Of/late-WN stars in LMC, R127 (HDE 269 858), to LBV phase (Stahl et al. 1983; Stahl & Wolf 1986; Wolf et al. 1988). Conversely, Galactic LBV AG Carinae manifested an Of/late-WN spectrum in its light minimum state (Stahl 1986). Subsequently, the relationship of the two classes was extended by a number of Of/late-WN stars which turned out to be LBVs or LBV candidates with Of/late-WN spectra: He 3-591 in our Galaxy; HD 5980 in SMC; R127, R71, HDE 269 582 in LMC; AF And, Var 15 in M31; and Var B, Var 2, MCA-1B, V532 in M33. It has been even assumed that Of/late-WN stars are quiescent LBVs and perhaps all LBVs in their hot state are Of/late-WN objects (Bohannon & Walborn 1989). During our spectral monitoring of the object we noted the variation of one of the distinctive lines for Of/late-WN stars He II 4686: it significantly weakened from 2012 to 2019 and then strengthened again from 2019 to 2020 and 2021. Similar behavior with disappearing He II 4686 line was demonstrated by two Of/late-WN stars, R127 (Stahl et al. 1983) and HDE 269 582 (Stahl 1986), that subsequently were classified as LBVs (Walborn et al. 2017). This may point to typical LBV instability of the object.

Massey et al. (2006) pointed out that the object is an analog of the well known LBV star P Cygni. We also notice P Cygni profiles in the hydrogen, Fe III and He I lines and close matching of the spectrum to those of P Cygni and P Cygni-like LBV candidate MN112. This is indicative of the common nature of the objects and supports LBV classification of the J004341.84.

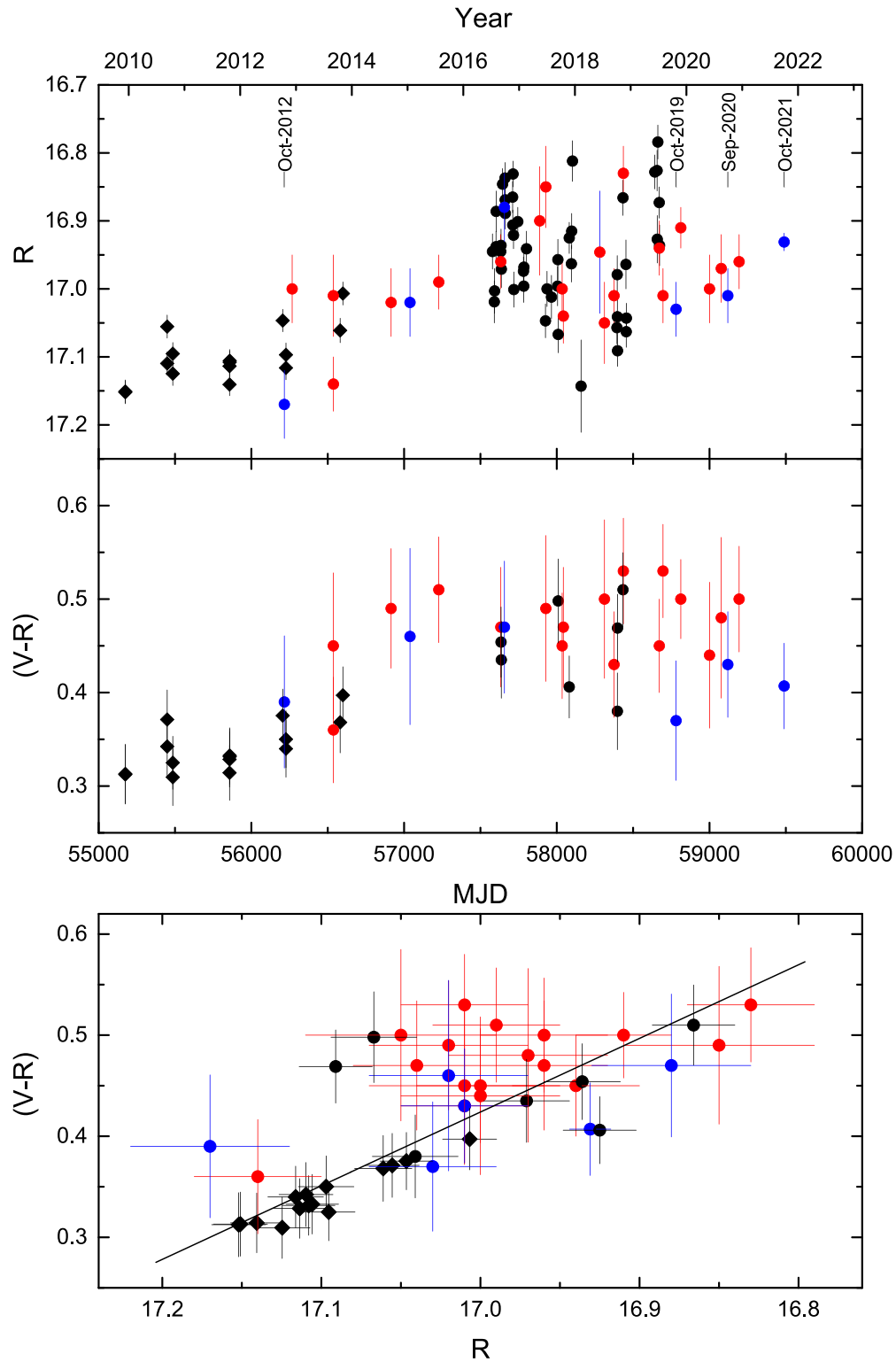


Figure 5. (Top) The R -band light curve together with the $(V - R)$ color plotted against Modified Julian Date (MJD) for J004341.84. The vertical lines indicate the dates of our spectra. (Bottom) The $(V - R)$ vs. R color-magnitude diagram of J004341.84. Black diamonds—data from Pan-STARRS (Chambers et al. 2016), red circles—data from Martin & Humphreys (2017), black circles—data from NAO Rozhen telescope, blue circles—BTA photometry.

We continue to apply a new method of LBV SED modeling (Sholukhova et al. 2015; Sarkisyan et al. 2020) to studying our LBV candidate. Our fitting of SEDs of several stellar states with constant extinction and bolometric luminosity yields $A_V = 1.98 \pm 0.07$ and $M_{\text{bol}} = -10.41 \pm 0.12$ mag. The obtained estimates of extinction and luminosity match those of Massey (2006) well, and the luminosity value corresponds to that of known LBVs in M31 (Humphreys et al. 2014). Estimated luminosity and temperature of J004341.84 put it in the immediate proximity of the S Dor instability strip (Wolf 1989) and remarkably close to P Cyg and R127 on the HR diagram.

The light curve of J004341.84 for the period from 2010 to 2020 displays variations of the order of 0.4 mag, with an overall brightness increasing trend $\Delta R > 0.1$ mag. In full accordance with the behavior of S Dor variables (Humphreys & Davidson 1994; Lamers et al. 1998; van Genderen 2001) the increase in brightness of the object corresponds to a redder color and therefore a cooler temperature.

Taking into account S Dor-type variability of the object and similarity of its spectrum and estimated luminosity to those of known LBVs, J004341.84 can be classified as an LBV star.

Acknowledgments

The reported study was funded by RFBR and NSFB according to the research project N 19-52-18007. Observations with the SAO RAS telescopes are supported by the Ministry of Science and Higher Education of the Russian Federation (including agreement No05.619.21.0016, project ID RFMEFI61919X0016). S.F., P.N. and A. Valcheva acknowledge partial support from the DN18-10/2017 grant from the NSF of Bulgaria. This work was performed with the equipment purchased from the funds of the Program of Development of Moscow University. The authors also thank the anonymous referee for their careful review and helpful suggestions that improved the manuscript.

ORCID iDs

A. Sarkisyan  <https://orcid.org/0000-0001-7320-2867>

References

- Afanasiev, V. L., & Moiseev, A. V. 2005, *AstL*, 31, 194
 Bohannan, B., & Walborn, N. R. 1989, *PASP*, 101, 520
 Chambers, K. C., Magnier, E. A., Metcalfe, N., et al. 2016, arXiv:1612.05560
 Cutri, R. M., Skrutskie, M. F., van Dyk, S., et al. 2012, VizieR Online Data Catalog: 2MASS 6X Point Source Working Database/Catalog, II/281
 Enoch, M. L., Brown, M. E., & Burgasser, A. J. 2003, *AJ*, 126, 1006
 Fitzpatrick, E. L. 1999, *PASP*, 111, 63
 Gvaramadze, V. V., Kniazev, A. Y., Fabrika, S., et al. 2010, *MNRAS*, 405, 520
 Humphreys, R. M., & Davidson, K. 1994, *PASP*, 106, 1025
 Humphreys, R. M., Davidson, K., Hahn, D., Martin, J. C., & Weis, K. 2017a, *ApJ*, 844, 40
 Humphreys, R. M., Gordon, M. S., Martin, J. C., Weis, K., & Hahn, D. 2017b, *ApJ*, 836, 64
 Humphreys, R. M., Weis, K., Davidson, K., Bomans, D. J., & Burggraf, B. 2014, *ApJ*, 790, 48
 Kostenkov, A., Fabrika, S., Sholukhova, O., Sarkisyan, A., & Bizyaev, D. 2020, *MNRAS*, 496, 5455
 Lamers, H. J. G. L. M., Bastiaanse, M. V., Aerts, C., & Spoon, H. W. W. 1998, *A&A*, 335, 605
 Leggett, S. K., Currie, M. J., Varricatt, W. P., et al. 2006, *MNRAS*, 373, 781
 Martin, J. C., & Humphreys, R. M. 2017, *AJ*, 154, 81
 Massey, P. 2006, *ApJL*, 638, L93
 Massey, P., McNeill, R. T., Olsen, K. A. G., et al. 2007, *AJ*, 134, 2474
 Massey, P., Neugent, K. F., & Smart, B. M. 2016a, *AJ*, 152, 62
 Massey, P., Neugent, K. F., & Smart, B. M. 2016b, VizieR Online Data Catalog: Revised LGGs UBVR1 photometry of M31 and M33 stars, J/AJ/152/62
 Massey, P., Olsen, K. A. G., Hodge, P. W., et al. 2006, *AJ*, 131, 2478
 Nadjip, A. E., Tatarnikov, A. M., Toomey, D. W., et al. 2017, *AstBu*, 72, 349
 Rafiei Ravandi, M., Barmby, P., Ashby, M. L. N., et al. 2016, *MNRAS*, 459, 1403
 Riess, A. G., Fliri, J., & Valls-Gabaud, D. 2012, *ApJ*, 745, 156
 Rose, M. B., & Hintz, E. G. 2007, *AJ*, 134, 2067
 Sarkisyan, A., Sholukhova, O., Fabrika, S., et al. 2020, *MNRAS*, 497, 687
 Sarkisyan, A. N., Vinokurov, A. S., Solovieva, Y. N., et al. 2017, *AstBu*, 72, 486
 Shatsky, N., Belinski, A., Dodin, A., et al. 2020, in Ground-Based Astronomy in Russia. 21st Century, ed. I. I. Romanyuk, I. A. Yakunin, A. F. Valeev, & D. O. Kudryavtsev (Nizhniy Arkhyz: Special Astrophysical Observatory (SAO RAS) Russian Academy of Sciences) 127–32
 Sholukhova, O., Bizyaev, D., Fabrika, S., et al. 2015, *MNRAS*, 447, 2459
 Sholukhova, O. N., Fabrika, S. N., Zharova, A. V., Valeev, A. F., & Goranskij, V. P. 2011, *AstBu*, 66, 123
 Simons, D. A., & Tokunaga, A. 2002, *PASP*, 114, 169
 Smith, N., Aghakhanloo, M., Murphy, J. W., et al. 2019, *MNRAS*, 488, 1760
 Stahl, O. 1986, *A&A*, 164, 321
 Stahl, O., Mandel, H., Wolf, B., et al. 1993, *A&AS*, 99, 167
 Stahl, O., & Wolf, B. 1986, *A&A*, 154, 243
 Stahl, O., Wolf, B., Klare, G., et al. 1983, *A&A*, 127, 49
 Stetson, P. B. 1987, *PASP*, 99, 191
 Stetson, P. B., Davis, L. E., & Crabtree, D. R. 1990, in ASP Conf. Ser. 8, CCDs in Astronomy, ed. G. H. Jacoby (San Francisco, CA: ASP), 289
 Tody, D. 1986, Proc. SPIE, 627, 733
 Tody, D. 1993, in ASP Conf. Ser. 52, Astronomical Data Analysis Software and Systems II, ed. R. J. Hanisch, R. J. V. Brissenden, & J. Barnes (San Francisco, CA: ASP), 173
 Tokunaga, A. T., Simons, D. A., & Vacca, W. D. 2002, *PASP*, 114, 180
 Tokunaga, A. T., & Vacca, W. D. 2005, *PASP*, 117, 421
 Tonry, J. L., Stubbs, C. W., Lykke, K. R., et al. 2012, *ApJ*, 750, 99
 van Genderen, A. M. 2001, *A&A*, 366, 508
 Walborn, N. R., Gamen, R. C., Morrell, N. I., et al. 2017, *AJ*, 154, 15
 Wolf, B. 1989, *A&A*, 217, 87
 Wolf, B., Stahl, O., Smolinski, J., & Casatella, A. 1988, *A&AS*, 74, 239